Clinical Neurophysiology 139 (2022) 1–8

Contents lists available at ScienceDirect

Clinical Neurophysiology

journal homepage: www.elsevier.com/locate/clinph

Assessing carpal tunnel syndrome with magnetoneurography

Toru Sasaki [a,*], Shigenori Kawabata [b], Jun Hashimoto [a], Yuko Hoshino [b], Kensuke Sekihara [b], Yoshiaki Adachi [c], Miho Akaza [d], Koji Fujita [e], Akimoto Nimura [e], Toshitaka Yoshii [a], Yuki Miyano [f], Yuki Mitani [f], Taishi Watanabe [f], Shinji Sato [f], Sukchan Kim [f], Atsushi Okawa [a]

[a] *Department of Orthopedic Surgery, Tokyo Medical and Dental University, 1-5-45 Yushima, Bunkyo-ku, Tokyo 113-8510, Japan*
[b] *Department of Advanced Technology in Medicine, Graduate School of Tokyo Medical and Dental University, 1-5-45 Yushima, Bunkyo-ku, Tokyo 113-8510, Japan*
[c] *Applied Electronics Laboratory, Kanazawa Institute of Technology, Kanazawa-shi, Ishikawa 920-1331, Japan*
[d] *Respiratory and Nervous System Science, Biomedical Laboratory Science, Graduate School of Tokyo Medical and Dental University, 1-5-45 Yushima, Bunkyo-ku, Tokyo 113-8510, Japan*
[e] *Department of Functional Joint Anatomy, Graduate School of Medical and Dental Sciences, Tokyo Medical and Dental University, 1-5-45, Yushima, Bunkyo-ku, Tokyo 113-8510, Japan*
[f] *Healthcare Business Group, Ricoh Company, Ltd., 2-3-10 Kandasurugadai Chiyoda-ku, Tokyo 101-0062, Japan*

ARTICLE INFO

Article history:
Accepted 30 March 2022
Available online 9 April 2022

Keywords:
Magnetoneurography
Carpal tunnel syndrome
Median nerve
Digital nerve
Conduction velocity
Nerve conduction study

HIGHLIGHTS

- Neural activity in carpal tunnel syndrome patients could be visualized using magnetoneurography.
- The lesion site could be visualized using the amplitude or nerve conduction velocity.
- Magnetoneurography could also visualize the improvement after surgery.

ABSTRACT

Objective: To measure the neuromagnetic fields of carpal tunnel syndrome patients after electrical digital nerve stimulation and evaluate median nerve function with high spatial resolution.
Methods: A superconducting quantum interference device magnetometer system was used to record neuromagnetic fields at the carpal tunnel after electrical stimulation of the middle digital nerve in 10 hands of nine patients with carpal tunnel syndrome. The patients were diagnosed based on symptoms (numbness, tingling, and pain) supported by a positive Phalen or Tinel sign. A novel technique was applied to remove stimulus-induced artifacts, and current distributions were calculated using a spatial filter algorithm and superimposed on X-ray.
Results: In 6 of the 10 hands, the amplitude of the inward current waveform attenuated to <70% or the nerve conduction velocity was <40 m/s. The results of conventional nerve conduction studies were normal for two of these six hands. All four hands that could not be diagnosed by magnetoneurography had severe carpal tunnel syndrome superimposed on peripheral neuropathy secondary to comorbidities.
Conclusions: Technical improvements enabled magnetoneurography to noninvasively visualize the electrophysiological nerve activity in carpal tunnel syndrome patients.
Significance: Magnetoneurography may have the potential to contribute to the detailed diagnosis of various peripheral nerve disorders.

Abbreviations: CSP, common-mode subspace projection; CTS, carpal tunnel syndrome; MNG, magnetoneurography; NCS, nerve conduction study; SQUID, superconducting quantum interference device; UGRENS, unit gain constraint recursively applied null-steering spatial filtering.

* Corresponding author at: Department of Orthopedic Surgery, Tokyo Medical and Dental University, 1-5-45 Yushima, Bunkyo-ku, Tokyo 113-8510, Japan.
E-mail addresses: t-sasaki.orth@tmd.ac.jp (T. Sasaki), kawabata.orth@tmd.ac.jp (S. Kawabata), hash.orth@tmd.ac.jp (J. Hashimoto), hoshino.atm@tmd.ac.jp (Y. Hoshino), k-sekihara@nifty.com (K. Sekihara), mihonuro@tmd.ac.jp (M. Akaza), fujiorth@tmd.ac.jp (K. Fujita), nimura.orj@tmd.ac.jp (A. Nimura), yoshii.orth@tmd.ac.jp (T. Yoshii), yuki.yh.hasegawa@jp.ricoh.com (Y. Miyano), yuuki.ym.mitani@jp.ricoh.com (Y. Mitani), taishi.watanabe@jp.ricoh.com (T. Watanabe), shinji.s1.satoh@jp.ricoh.com (S. Sato), sukchan.kim@jp.ricoh.com (S. Kim), okawa.orth@tmd.ac.jp (A. Okawa).

https://doi.org/10.1016/j.clinph.2022.03.021
1388-2457/

1. Introduction

In carpal tunnel syndrome (CTS), the most common nerve entrapment syndrome, the median nerve is entrapped at the wrist. CTS is primarily diagnosed via history and physical examination, but objective electrophysiological evaluation can help to determine the indication for surgery and assess postoperative function. The sensitivity of median nerve distal motor latency ranges from 29% to 81% while that of wrist-palm sensory conduction velocity varies from 45% to 100% (Moon et al., 2017). Meanwhile, Yılmaz et al. (2017) determined the specificity of median nerve distal motor latency to be 99% and the sensitivity of wrist-digit sensory conduction velocity to be 97%. Nerve conduction studies (NCSs) sometimes obtain no abnormal findings, even when the hand surgeon suspects CTS (Buchthal et al., 1974; Sedal et al., 1973, Thomas et al., 1967). In these cases, it is sometimes difficult to select a patient's treatment method without objective evidence supporting invasive surgery. Moreover, the electrical potential recorded from the body surface is attenuated owing to a thick skin or transverse ligament (Werner and Andary, 2011).

In contrast to electrical potential recording from the body surface, the magnetic field is less affected by the surrounding bone and soft tissue and has theoretically higher resolution (Trahms et al., 1989). Our group has developed a novel method to visualize the distribution of neural currents in the peripheral nerve and spinal cord using measurement of the neuromagnetic field (Ishii et al., 2012; Sumiya et al., 2017; Ushio et al., 2019). We have also reported the visualization of the electrophysiological activity at the carpal tunnel area in response to stimulation of the digital nerve by neuromagnetic field measurement in healthy individuals using the common-mode subspace projection (CSP) method, which is a new method for removing stimulus-induced artifacts (Sasaki et al., 2020). In this study, we report for the first time the visualization of the electrophysiological nerve activity in CTS patients in response to stimulation of the digital nerve by magnetoneurography (MNG) from the body surface.

2. Methods

2.1. MNG system and measurement at the carpal tunnel area

This study was approved by the Ethics Committee of Tokyo Medical and Dental University and was performed in accordance with the Declaration of Helsinki with the written informed consent of participants. We included 10 hands of nine patients (mean age ± SD, 65.9 ± 12.6 years; three men, six women) with CTS (bilateral CTS, 1; unilateral CTS, 8) who were diagnosed by hand surgeons. The clinical diagnosis was based on symptoms of CTS (numbness, tingling, and pain) provoked or worsened by a sustained wrist position and relieved by shaking of the hands and a positive examination for CTS including a positive Phalen or Tinel sign. Patients who could not maintain the measurement posture or who had previously undergone a carpal tunnel release operation were excluded from this study.

All recordings were performed in a magnetically shielded room using a superconducting quantum interference device (SQUID) magnetometer system, developed by Kanazawa Institute of Technology and Ricoh Company, Ltd. (Adachi et al., 2017). Participants sat on a chair and placed their palm on the curve of the sensor surface, as in a previous report (Fig. 1a) (Sasaki et al., 2020). To obtain positional information on the hand and magnetic sensor during the measurement, lateral and frontal radiographs were taken while the patient was in the measurement position. The middle finger was electrically stimulated at the distal interphalangeal joint (square wave pulse; 3 Hz; 0.2 ms in duration) with over 2–3 times the sensory threshold (intensity, 6–18 mA). We chose the middle finger because previous research showed that the signal intensity was higher after middle finger stimulation than after index finger stimulation (Sasaki et al., 2020). The evoked magnetic fields after the stimulation of the middle finger were recorded at the surface of the palmar area under the following conditions: sampling rate, 40 kHz; bandpass filter, 100–5000 Hz; two thousand recordings (first measurement).

After the first measurement, to exclude stimulus-induced artifacts from the entire signals obtained by MNG in response to the electrical stimulation of the middle finger, we also measured the magnetic field of the stimulus-induced artifacts alone (second measurement). A 30-mm urethane plate was placed between the palm and the sensor surface with the same finger position as in the first measurement, and the nerve magnetic field was measured under the same conditions (Fig. 1b). In the second measurement, the distance between the sensor and the nerve at the palm area is increased, which reduces the signals from the nerve at the palm area, allowing isolation of the signals derived from the stimulus-induced artifacts alone.

2.2. Signal processing

First, we removed stimulus-induced artifacts from the acquired entire MNG signals of the first measurement by applying the CSP algorithm (Watanabe et al., 2013). The CSP algorithm is a novel method for calculating magnetic signals derived from neural activity alone using the first entire magnetic signals (neural signal + artifacts) and the second magnetic signals of the stimulus-induced

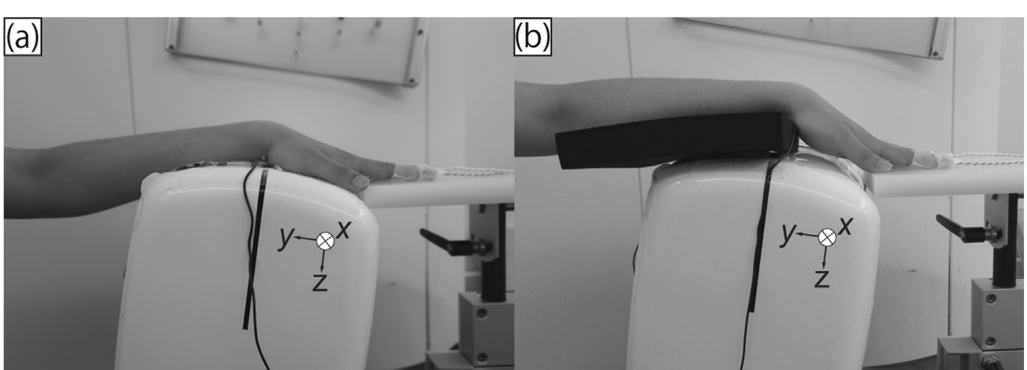

Fig. 1. Measurement methods for neuromagnetic fields. (a) Participants placed their palm on the curve of the sensor surface. We measured the neuromagnetic fields after electrical stimulation at the distal interphalangeal joint of the middle finger. (b) Measurement of the magnetic fields of stimulus-induced artifacts. A 30-mm urethane plate was placed between the palm and the sensor surface with the fingers in the same position.

artifacts. A spatial filter algorithm, unit gain constraint recursively applied null-steering spatial filtering (UGRENS), was applied to the magnetic signal derived from neural activity (artifact-removed magnetic signal), and this algorithm can calculate the temporal and spatial distributions of the currents (Sekihara and Nagarajan, 2015; Sasaki et al., 2020). The calculated currents were superimposed on the X-rays taken during the measurement. The distributions and intensities of the currents were visualized using a color map. In this method, we were able to calculate the current waveforms at arbitrary points as if virtual electrodes were placed there. We set the virtual electrodes along the digital and median nerves at 10-mm intervals. We calculated the current waveform perpendicular to the digital and median nerve at virtual electrode points. This current reflects the inward current at the depolarization points (Sasaki et al., 2020). The conduction velocity was also calculated from the apex of the latency in this inward current waveform. Because it has been shown that the propagation of the inward current stops at the lesion site in animal experimentation (Tomori et al., 2010), the lesion site was defined as the level at which the amplitude of the inward current of the depolarization point decreased below 70% compared with the next electrode or the level at which the conduction velocity calculated from the inward current waveform decreased below 40 m/s.

2.3. Nerve conduction study

A conventional NCS of the bilateral median nerve was performed using an evoked potential/electromyography system (MEB-2300; Nihon Kohden, Tokyo, Japan) with the bandpass filter set at 10 Hz to 5 kHz for motor nerve recording and at 20 Hz to 2 kHz for sensory recording. The compound muscle action potential was recorded with a pair of surface cup electrodes placed over the abductor pollicis brevis by using the belly-tendon method. Square-pulse supramaximal electrical stimuli at 0.5 Hz with a duration of 0.3 ms were delivered at the wrist and elbow. The wrist stimulation point was 7 cm proximal to the cathode electrode placed on the abductor pollicis brevis. The sensory nerve action potential of the median nerve was antidromically recorded with a pair of cup electrodes placed over the distal and proximal interphalangeal joints of the index finger. Square-pulse supramaximal electrical stimuli at 0.5 Hz with a duration of 0.3 ms were delivered at the palm, wrist, and elbow. Measurements included the peak-to-peak amplitude of the response, distal latency, and conduction velocity. Each measurement was performed twice to confirm reproducibility. Waveforms with unclear latency and no reproducibility were considered non-measurable.

Because the findings of the preoperative conventional NCS for Patient 5 were normal, we also intraoperatively recorded nerve potentials. During the surgery, we used a larger incision to identify the lesion site and performed adequate decompressions both distally and proximally. We electrically stimulated the median nerve percutaneously (square wave pulse; 5 Hz; 0.3 ms in duration) at the elbow immediately after decompression and recorded potentials every 1 cm at four locations directly above the nerve. The conduction velocity was calculated from the latency of each waveform and compared with the preoperative neuromagnetic field measurements. We also performed neuromagnetic field measurements again at 6 postoperative months in this case.

3. Results

The results are summarized in Table 1. Except for the right side of Patients 3 and 5, the NCSs indicated focal neuropathy at the carpal tunnel area. In 6 of the 10 hands, the amplitude of the inward current waveform calculated from the MNG results attenuated to

Table 1
Patients' demographic and clinical characteristics, NCS, and MNG results.

Patient	Age (years)	Sex	Affected side	Comorbidities	DML (ms)	SCV (m/s)	SNAP (μV)	Bland classification	MNG result
1	63	Male	Left		4	32.8	4.9	Grade 2 (mild)	The amplitude decreased at the middle level of the metacarpal bone
2	63	Male	Right		NE	NE	NE	Grade 6 (extremely severe)	Signal was too small to diagnose
3	54	Female	Right		3.1	56.5	73.8	Normal	Conduction velocity decreased at the base of the metacarpal bone
			Left		5.2	32.4	93.3	Grade 3 (moderately severe)	Conduction velocity decreased at the middle level of the metacarpal bone
4	79	Female	Right	Diabetes, rheumatoid arthritis	3.7	35	6.5	Grade 2 (mild)	Signal was too small to diagnose
5	62	Female	Right	Cervical extramedullary tumor	2.9	59.2	54.6	Normal	Conduction velocity decreased at the base of the metacarpal bone
6	79	Male	Left	Cervical myelopathy	4.7	36.7	23.6	Grade 3 (moderately severe)	The amplitude decreased at the middle level of the metacarpal bone
7	43	Female	Left		4	36.1	37.4	Grade 2 (mild)	The amplitude decreased at the middle level of the metacarpal bone
8	81	Female	Left	Hemodialysis, diabetes	7.6	14.2	2.6	Grade 3 (moderately severe)	Signal was too small to diagnose
9	69	Female	Right	Hemodialysis	5.8	20.1	2.8	Grade 3 (moderately severe)	Signal was too small to diagnose

DML, distal motor latency; MNG, magnetoneurography; NE, not evoked; SCV, sensory nerve conduction velocity (palm to wrist); SNAP, sensory nerve action potential.

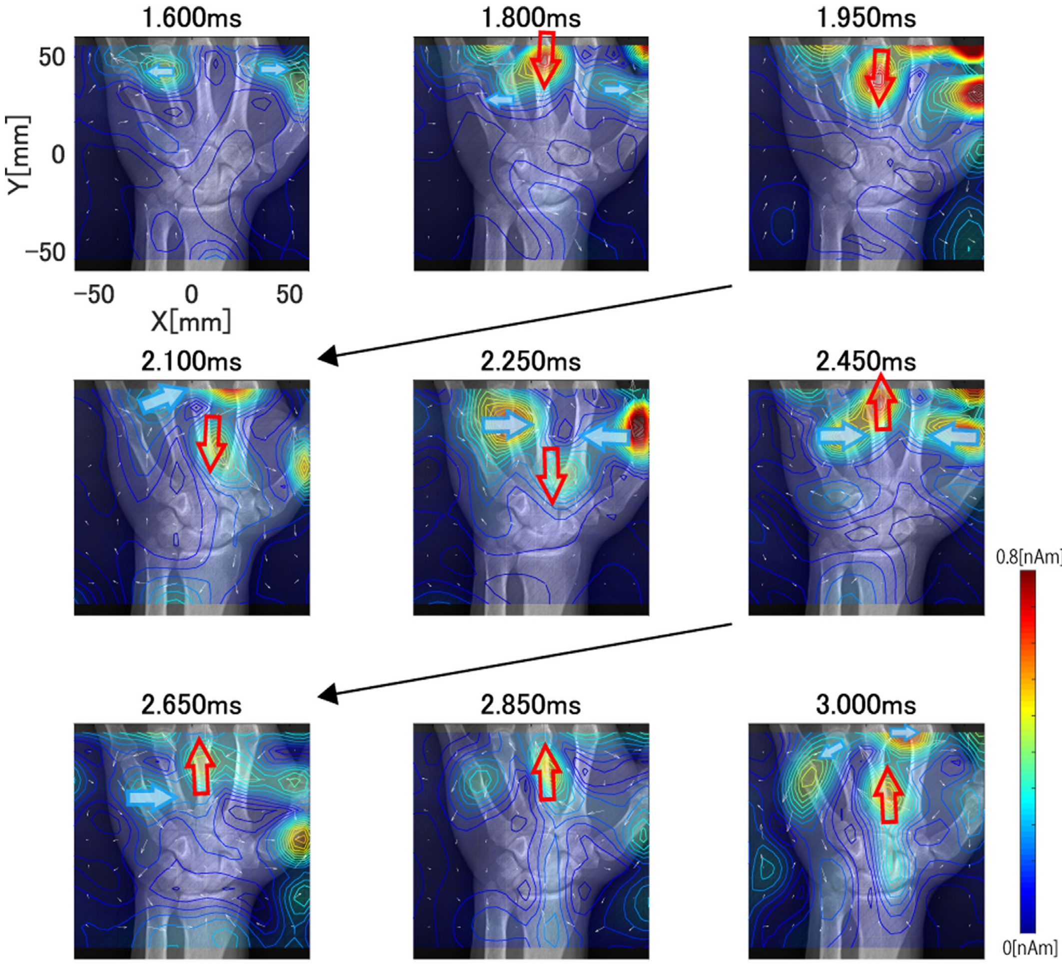

Fig. 2. Calculated currents of Patient 1. Calculated current maps superimposed on an X-ray image. Current intensity is shown by a color scale (red is higher). The small white arrows indicate current vectors. The leading currents (downward-pointing red arrows), trailing currents (upward-pointing red arrows), inward currents (large blue arrows), and outward currents (small blue arrows) propagated in the distal to proximal direction along the median nerve. However, the inward currents attenuated at the middle level of the metacarpal bone of the middle finger.

less than 70% or the nerve conduction velocity was less than 40 m/s. The results of conventional NCSs were normal (Bland, 2000) for two of these six hands (right hands of Patients 3 and 5) but they showed an abnormal pattern at the base of the metacarpal bone on MNG. In the remaining four hands (Patient 1 and the left hands of Patients 3, 6, and 7), the MNG results showed an abnormal pattern at the central level of the metacarpal bone. The four hands (Patients 2, 4, 8, and 9) that could not be diagnosed by MNG were those of patients with severe CTS or comorbidities. These hands were found to have too small a neuromagnetic field signal to obtain detailed information on the level of the lesion site.

Fig. 2 shows the result of Patient 1, who had Bland classification grade 2 (Table 1). The reconstructed currents comprised a leading current, a trailing current, and an inward/outward current. All currents showed an attenuated intensity at the center of the metacarpal bone of the middle finger (Fig. 2). We placed virtual electrodes along the median nerve and calculated the waveforms for the inward current. The amplitude of waveform 7 decreased to about 36.9% of that of waveform 8 (Fig. 3).

Fig. 4 shows the result of Patient 5, who had a normal result on the NCS (Table 1). The reconstructed currents after stimulation of the middle finger comprised leading, trailing, and inward/outward currents. All currents propagated from distal to proximal without intensity attenuation (Fig. 4). In the calculated inward current waveforms, only parts of waveforms 8 to 7, 7 to 6, and 6 to 5 showed reduced conduction velocities of 37.35, 27.51, and 38.00 m/s, respectively (Fig. 5a). The mean conduction velocity of all waveforms (waveforms 9 to 1) was normal (46.3 m/s).

We intraoperatively measured nerve action potentials to check for conduction block (Fig. 5b). During surgery, the median nerve was found to be erythematous and flattened on the distal side of the transverse carpal ligament. Measurement of nerve action potentials revealed a local conduction delay in this area, which was consistent with the results of preoperative MNG (Fig. 5). We repeated the magnetic field measurement 6 months after the surgery when her numbness had improved (Fig. 6). The calculated inward current waveforms showed a healthy pattern.

4. Discussion

In this study, we were able to measure neuromagnetic fields at the carpal tunnel area after stimulation of the digital nerve and visualize the detailed distribution and propagation of the electrophysiological nerve activity in CTS patients.

Although various sensors have been used to measure the magnetic fields of human peripheral nerves (Trahms et al., 1989; Wikswo et al., 1990; Hoshiyama et al., 1999; Mackert, 2004;

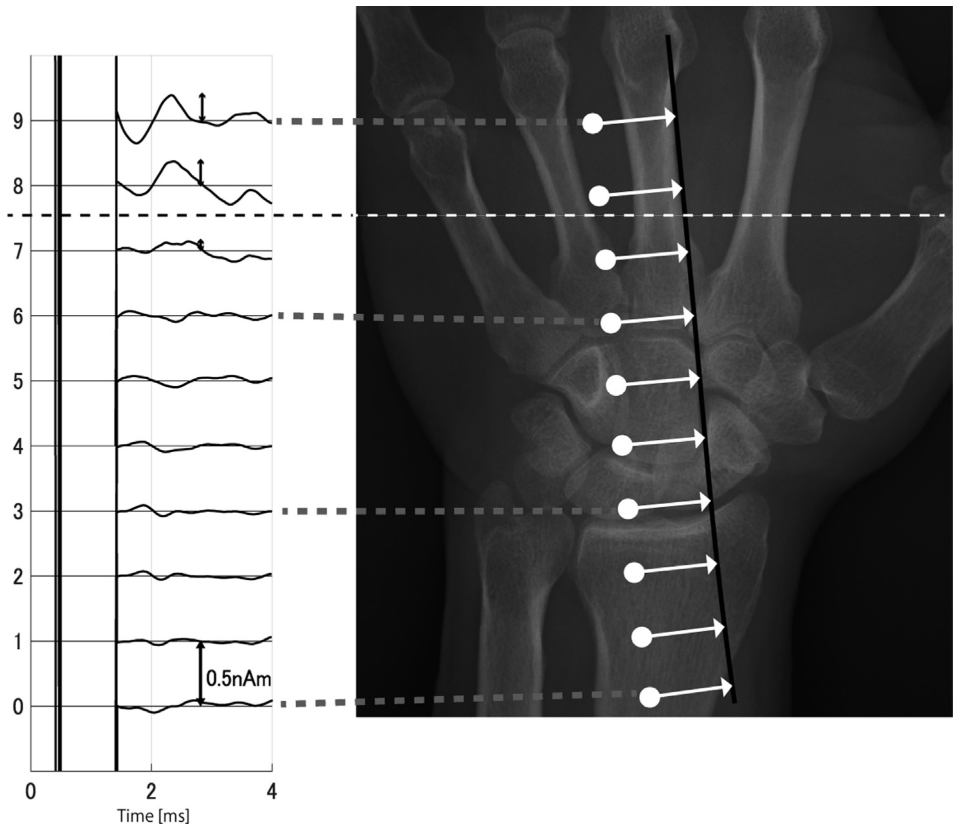

Fig. 3. The waveforms of the calculated currents at the "virtual electrodes" (white circle) 15 mm lateral from the nerve pathway (upward is toward the nerve pathway). The peaks in waveforms are equivalent to the inward currents at the depolarization point. Although the waveforms conducted in the distal to proximal direction, the amplitude of waveform 7 decreased to about 36.9% of that of waveform 8 at the middle level of the metacarpal bone of the middle finger.

Nakanishi et al., 2004), there has been no report of magnetic field measurement at the carpal tunnel area from the body surface. We successfully measured neuromagnetic fields and visualized the detailed distribution of the electrophysiological nerve activity in 6 of the 10 patients with CTS using MNG. These results suggest that our method may be able to visualize local conduction disturbances in patients with mild peripheral neuropathy. In addition, two types of lesion sites were indicated from the reconstructed current waveform: one was found at the central level of the metacarpal bone and the other was found at the base of the metacarpal bone. A lesion site with waveform changes at the central level of the metacarpal bone may indicate that the neuropathy extends distally to the entrapment area. However, in this study, we were not able to identify the true lesion site of the neuropathy by other methods (except in Patient 5, when the intraoperative neurophysiology was assessed), so we were unable to elucidate the pathogenesis of the waveform changes at distal areas.

In the other four cases (Patients 2, 4, 8, and 9), we were unable to measure neuromagnetic fields in detail because the neuromagnetic field signal was small. Patient 2 was a severe case that was non-measurable in a conventional NCS, and the neuromagnetic field signal after stimulation of the digital nerve was believed to be insufficient. Although Patient 4 had a mild case of CTS with electrophysiological severity scale grade 2, the neuromagnetic field signal might be small due to peripheral neuropathy associated with comorbid diabetes mellitus and rheumatoid arthritis. Patients 8 and 9 were long-term hemodialysis patients with delayed sensory nerve conduction velocities of 14.2 m/s and 20.1 m/s in the digit-palm segment, and neuropathy was observed not only in the palm-wrist segment, but also in the distal part. In these cases, the number of fibers that could be stimulated by finger stimulation was too small for visualization of the electrophysiological nerve activity. These results show that the neuromagnetic field signal may be small in patients with severe peripheral neuropathy, patients undergoing hemodialysis, and patients with diabetes.

For Patient 5, we repeated the measurement 6 months after the surgery and confirmed that the local conduction disturbance had disappeared. This method may contribute to preoperative and postoperative electrophysiological evaluations. There have been some reports of patients whose symptoms worsened after surgery for CTS (Bland, 2007). Therefore, the ability to perform such a detailed electrophysiological evaluation with leading and trailing intra-axonal currents and inward/outward currents before and after the surgery may help to identify the cause of poor results and predict prognosis.

There are several limitations to this study. The first is that there were few cases. We need to accumulate and analyze a large number of cases to demonstrate the sensitivity, specificity, and effectiveness of MNG. Second, this system is a newer device that requires costly magnetic sensors and shielded rooms and has problems associated with a high stimulation frequency and long examination time.

5. Conclusion

In this study, we successfully measured neuromagnetic fields after finger nerve stimulation and visualized the detailed distribution of the electrophysiological nerve activity in patients with CTS through technical improvements involving the removal of stimulus-induced artifacts and source analysis. The decrease in the intensity of the inward current at the depolarization area and

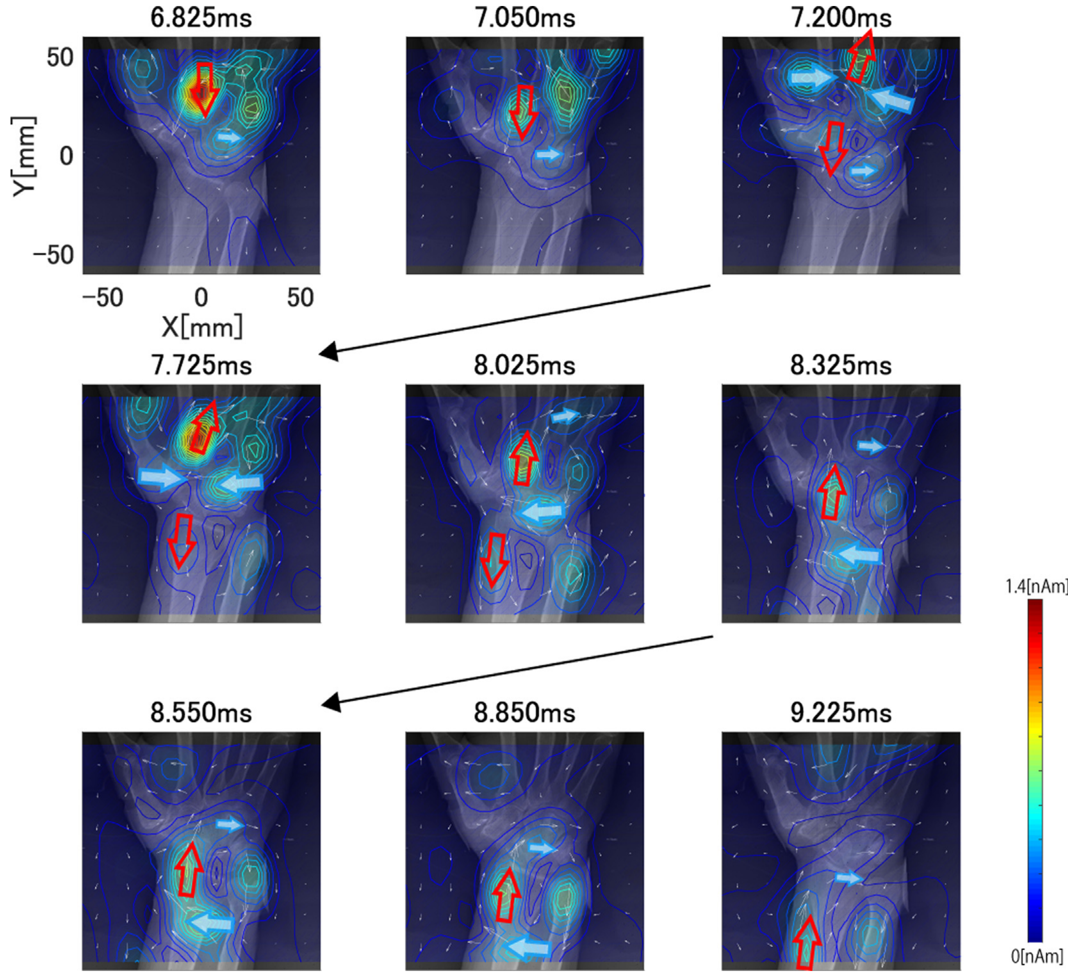

Fig. 4. Calculated currents of Patient 5. Currents are illustrated in a similar manner to those in Fig. 2. The leading, trailing, and inward currents propagated in the distal to proximal direction along the median nerve.

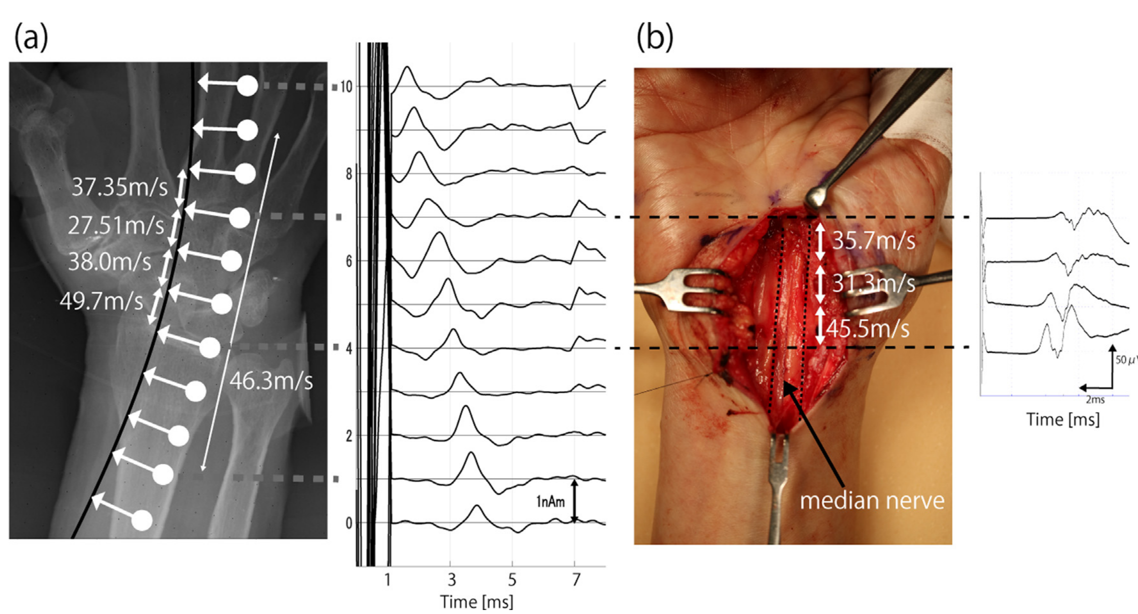

Fig. 5. Waveforms of calculated currents at the "virtual electrodes" and compound nerve action potentials (CNAPs) in response to median nerve stimulation at the elbow. (a) Currents at virtual electrodes (white circle) 15 mm lateral from the nerve pathway. The currents are illustrated in a similar manner to those in Fig. 3. The amplitudes of the inward current waveforms did not attenuate. Conduction velocity was delayed only in the carpal tunnel area with conduction velocities of 37.35, 27.52, and 38.00 m/s in waveforms 8 to 7, 7 to 6, and 6 to 5, respectively. (b) Intraoperative CNAPs. Similar to the results of preoperative MNG, the CNAPs also showed focal conduction disturbances in the carpal tunnel area. CNAPs, compound nerve action potentials; MNG, magnetoneurography.

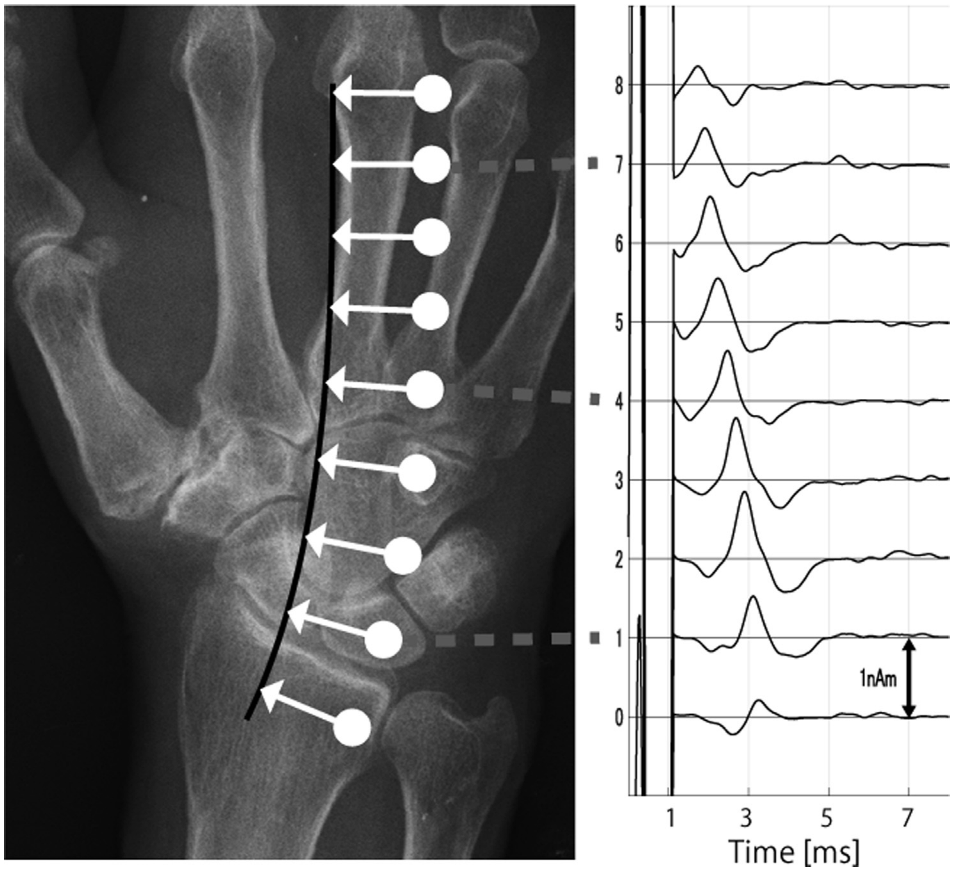

Fig. 6. Waveforms of calculated currents at the "virtual electrodes" along the median nerve (Patient 5) at 6 postoperative months. Currents are illustrated in a similar manner to those in Fig. 3. The current waveform showed a normal conduction pattern 6 months after the surgery.

the decrease in conduction velocity reflected median nerve neuropathy in the carpal tunnel area. MNG may have the potential to contribute to the evaluation of various peripheral nerve disorders in the future.

Funding

This research was supported by Ricoh Company, Ltd. The funding body played no role in study design, data collection and analysis, preparation of the manuscript, or the decision to publish.

CRediT authorship contribution statement

T.S., S. Kawabata, and A.O. took part in the Conceptualization and Methodology; T.S., S. Kawabata, J.H., Y.H., M.A., K.F., A.N., T. Y., Y.A., Y. Miyano, Y. Mitani, T.W., S.S., S. Kim, and K.S. carried out Data curation and Formal analysis; T.S., S. Kawabata, J.H., Y. Miyano, Y. Mitani, T.W., S.S., S. Kim, and Y.A. developed the Software; S. Kawabata contributed Funding acquisition, T.S. contributed to Writing and S. Kawabata and A.O. contributed to review & editing.

Declaration of Competing Interest

The authors declare that they have no known competing financial interests or personal relationships that could have appeared to influence the work reported in this paper.

References

Adachi Y, Kawabata S, Fujihira J, Uehara G. Multi-channel SQUID magnetospinogram system with closed-cycle helium recondensing. IEEE Trans Appl Supercond 2017;27:1–4. https://doi.org/10.1109/TASC.2016.2631422.

Bland JD. A neurophysiological grading scale for carpal tunnel syndrome. Muscle Nerve 2000;23:1280–3. https://doi.org/10.1002/1097-4598(200008)23:8<1280::aid-mus20>3.0.co;2-y.

Bland JD. Treatment of carpal tunnel syndrome. Muscle Nerve 2007;36:167–71. https://doi.org/10.1002/mus.20802.

Buchthal F, Rosenfalck A, Trojaborg W. Electrophysiological findings in entrapment of the median nerve at wrist and elbow. J Neurol Neurosurg Psychiatry 1974;37:340–60. https://doi.org/10.1136/jnnp.37.3.340.

Hoshiyama M, Kakigi R, Nagata O. Peripheral nerve conduction recorded by a micro gradiometer system (micro-SQUID) in humans. Neurosci Lett 1999;272:199–202. https://doi.org/10.1016/s0304-3940(99)00589-3.

Ishii S, Kawabata S, Tomizawa S, Tomori M, Sakaki K, Shinomiya K, Sekihara K, Sato T, Adachi Y, Okawa A. Conductive neuromagnetic fields in the lumbar spinal canal. Clin Neurophysiol 2012;123(8):1656–61.

Mackert BM. Magnetoneurography: theory and application to peripheral nerve disorders. Clin Neurophysiol 2004;115:2667–76. https://doi.org/10.1016/j.clinph.2004.07.028.

Moon PP, Maheshwari D, Sardana V, Bhushan B, Mohan S. Characteristics of nerve conduction studies in carpal tunnel syndrome. Neurol India 2017;65(5):1013–6. https://doi.org/10.4103/neuroindia.NI_628_16.

Nakanishi K, Mashiko T, Fujimoto Y, Tanaka N, Iwase Y, Ishida O, Ochi M. Wide-range visualization of compound nerve action magnetic fields in the human median and ulnar nerves from the forearm to Erb's point. Neurosci Lett 2004;356(2):151–3.

Sasaki T, Kawabata S, Hoshino Y, Sekihara K, Adachi Y, Akaza M, Ozaki I, Fujita K, Nimura A, Yoshii T, Miyano Y, Mitani Y, Watanabe T, Sato S, Kim S, Okawa A. Visualization of electrophysiological activity at the carpal tunnel area using magnetoneurography. Clin Neurophysiol 2020;131(4):951–7.

Sedal L, McLeod JG, Walsh JC. Ulnar nerve lesions associated with the carpal tunnel syndrome. J Neurol Neurosurg Psychiatry 1973;36:118–23. https://doi.org/10.1136/jnnp.36.1.118.

Sekihara K, Nagarajan SS, editors. Electromagnetic brain imaging: a Bayesian perspective. Cham: Springer International Publishing; 2015.

Sumiya S, Kawabata S, Hoshino Y, Adachi Y, Sekihara K, Tomizawa S, Tomori M, Ishii S, Sakaki K, Ukegawa D, Ushio S, Watanabe T, Okawa A. Magnetospinography visualizes electrophysiological activity in the cervical spinal cord. Sci Rep 2017;7(1). https://doi.org/10.1038/s41598-017-02406-8.

Thomas JE, Lambert EH, Cseuz KA. Electrodiagnostic aspects of the carpal tunnel syndrome. Arch Neurol 1967;16:635–41. https://doi.org/10.1001/archneur.1967.00470240073010.

Tomori M, Kawabata S, Tomizawa S, Ishii S, Enomoto M, Adachi Y, Sato T, Shinomiya K, Okawa A. Diagnosis of incomplete conduction block of spinal cord from skin surface using spinal cord evoked magnetic fields. J Orthop Sci 2010;15(3):371–80.

Trahms L, Erne SN, Trontelj Z, Curio G, Aust P. Biomagnetic functional localization of a peripheral nerve in man. Biophys J 1989;55:1145–53. https://doi.org/10.1016/S0006-3495(89)82911-X.

Ushio S, Hoshino Y, Kawabata S, Adachi Y, Sekihara K, Sumiya S, Ukegawa D, Sakaki K, Watanabe T, Hasegawa Y, Okawa A. Visualization of the electrical activity of the cauda equina using a magnetospinography system in healthy subjects. Clin Neurophysiol 2019;130(1):1–11.

Watanabe T, Ukegawa D, Kawabata S, Adachi Y, Sekihara K. Removal of stimulus-induced artifacts in functional spinal cord imaging. 2013 35th Annual International Conference of the IEEE Engineering in Medicine and Biology Society (EMBC). Osaka, Japan; July 3–7, 2013.

Werner RA, Andary M. Electrodiagnostic evaluation of carpal tunnel syndrome. Muscle Nerve 2011;44:597–607. https://doi.org/10.1002/mus.22208.

Wikswo JP, Henry WP, Friedman RN, Kilroy AW, Wijesinghe RS, van Egeraat JM, et al. Intraoperative recording of the magnetic field of a human nerve. In: Williamson SJ, Hoke M, Stroink G, Kotani M, editors. Advances in biomagnetism. Boston, MA: Springer; 1990. p. 137–40.

Yılmaz F, Gündüz OH, Akyüz G. Lumbrical-interosseous recording technique versus routine electrodiagnostic methods in the diagnosis of carpal tunnel syndrome. Turkish J Phys Med Rehabil 2017;63(3):230–8. https://doi.org/10.5606/tftrd.2017.311.